NASA
Technical
Paper
2862

1988

High-Pressure Calorimeter Chamber Tests for Liquid Oxygen/Kerosene (LOX/RP-1) Rocket Combustion

Philip A. Masters,
Elizabeth S. Armstrong,
and Harold G. Price
Lewis Research Center
Cleveland, Ohio

National Aeronautics
and Space Administration

Scientific and Technical
Information Division

Summary

An experimental program was conducted to investigate the rocket combustion and heat transfer characteristics of liquid oxygen/kerosene (LOX/RP-1) mixtures at high chamber pressures. Two water-cooled calorimeter chambers of different combustion lengths were tested using 37- and 61-element oxidizer-fuel-oxidizer triplet injectors. The tests were conducted at nominal chamber pressures of 4.1, 8.3, and 13.8 MPa abs (600, 1200, and 2000 psia). Heat flux Q/A data were obtained for the entire calorimeter length for oxygen/fuel mixture ratios of 1.8 to 3.3. Test data at 4.1 MPa abs compared favorably with previous test data from another source. Using an injector with a fuel-rich outer zone reduced the throat heat flux by 47 percent with only a 4.5 percent reduction in the characteristic exhaust velocity efficiency C^*_{eff}. The throat heat transfer coefficient was reduced approximately 40 percent because of carbon deposits on the chamber wall.

Introduction

Preliminary design studies (refs. 1 to 4) by NASA and its contractors for vehicles such as the mixed-mode single-stage-to-orbit and the heavy lift launch vehicle have shown a need for a new high-pressure rocket engine using liquid oxygen (LOX) and hydrocarbon fuels as the propellants. Since early work with hydrocarbon-fueled rocket engines was done mostly at low chamber pressures, very little fundamental combustion and heat transfer data exist for the liquid oxygen/hydrocarbon propellant combinations at higher pressures. Major concerns for new propulsion systems include combustion efficiency and stability, cooling techniques, and heat transfer on the hot-gas side of the engine.

Analysis and testing have been done (ref. 5) to determine whether high performance could be achieved with stable combustion of heavy hydrocarbon fuels. The test series used three representative hydrocarbon fuels for combustion: RP-1 (kerosene), JP-10, and liquefied natural gas (more than 90 percent methane). Results showed that heavier hydrocarbons, such as JP-10 and RP-1, can provide high combustion efficiency with stable combustion; almost as high as with lighter hydrocarbons, such as liquefied natural gas. Other work has been done (refs. 6 and 7) to determine the cooling techniques that would be necessary for the chamber walls to withstand high combustion temperatures and to combat possible carbon deposition in the cooling channels. Cooling with heavy hydrocarbons at high pressures can cause formation of carbon deposits in the cooling channels (coking), thereby resulting in decreased heat transfer to the coolant and increased pressure drop in the coolant. As a result, other cooling concepts have been studied; for example, cooling the engine with oxygen (ref. 6) or applying a thermal barrier on the hot-gas side (ref. 7). Analysis on such thermal barriers as ceramic coatings, film cooling, and zoned combustion (ref. 7) determined that zoned combustion needs experimental verification for use in liquid oxygen/hydrocarbon rocket engines. Zoned combustion reduces the wall heat flux by using a mixture ratio below nominal on the outer zone of injector elements and a mixture ratio above nominal in the other injector elements. In experimental work with zoned liquid oxygen/hydrogen combustion, a 3-percent performance loss in a nonoptimal injector resulted in an 11-percent reduction in heat flux. Zoned liquid oxygen/hydrocarbon combustion had not been experimentally tested previous to this test series.

Investigative work (ref. 8) determined that RP-1 should be the preferred hydrocarbon for use at high chamber pressures because of its favorable density and specific impulse as well as its projected cost and safety considerations. Subsequent experimental work (ref. 9) investigated the heat transfer on the hot-gas side of the engine with RP-1 as the rocket fuel. The experimental testing of reference 9 produced fundamental combustion and heat transfer data at high chamber pressures. These data indicate a heat flux at the throat 70 percent greater than predicted, thereby demonstrating the need for better heat transfer calculation methods and more testing.

Because zoned combustion looks promising analytically for reducing heat flux to the chamber wall, zoned combustion should be verified experimentally. Also, more fundamental heat transfer data are needed to determine heat flux trends and to improve heat transfer calculation methods before RP-1 can be used for a high-pressure rocket engine. The program reported herein included testing for these purposes.

The objectives of this experimental program were (1) to obtain hot-gas-side heat transfer data at high chamber pressures and compare the results with those of reference 9, (2) to evaluate thrust chamber configurations with zoned combustion, and (3) to compare heat transfer data for zoned combustion with data for uniform combustion.

Symbols

A	area, cm^2
C	specific heat, kJ/(kg K)
C^*	characteristic exhaust velocity, cm/s
d	hydraulic diameter of the coolant passages, cm
G	mass velocity of the propellant flow, $kg/(cm^2\ s)$
h	heat transfer coefficient, $W/(cm^2\ K)$
k	average thermal conductivity, W/(cm K)
$\dot{m}$	mass flowrate, kg/s
O/F	mixture ratio of oxygen to fuel
P_C	chamber pressure, MPa abs
Pr	Prandtl number
Q	rate of heat transfer, kW
R	resistance, $(K\ cm^2)/W$
Re	Reynolds number
T	temperature, K
X	metal thickness, cm
δ	recovery factor

Subscripts:

a	adiabatic
c	coolant
d	carbon deposit
e	exit
eff	efficiency
f	function of film temperature
g	combustion gas
i	inlet
k	core
m	metal
o	total
ODE	one-dimensional equilibrium
p	function of pressure
s	static
UMR	uniform mixture ratio
w	wall
z	barrier zone

Superscripts:

$'$	combined zone and core flow

Apparatus

Chamber

Figure 1 is a schematic of the overall test assembly showing the hardware components, flow arrangement, and instrumentation. The major hardware components include the calorimeter

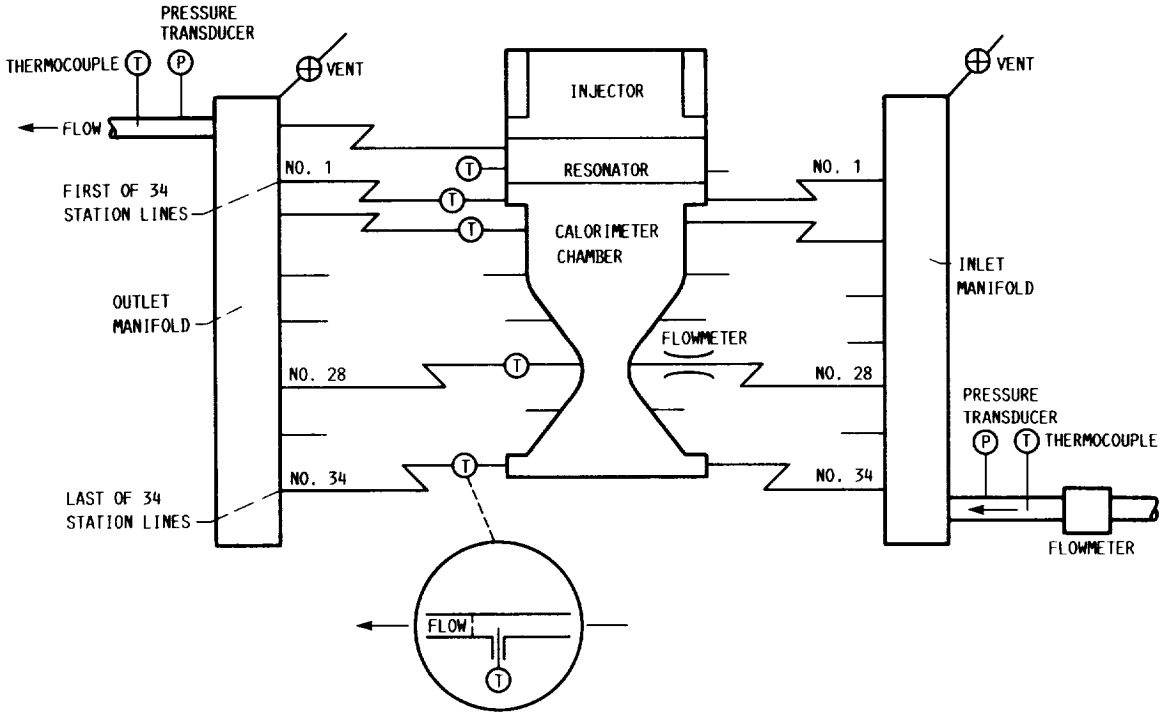

Figure 1.—Calorimeter chamber flow and instrumentation schematic.

chamber, a water-cooled resonator (located at the front of the injector body), and the injector. The two water-cooled calorimeter chambers were fabricated from oxygen-free, high-conductivity copper liners with machined circumferential coolant passages. The passages were closed out with 0.50 cm (0.20 in.) of electroformed nickel as the outer wall of the chamber.

The chamber dimensions in figure 2 show the half angle of 15° beyond the throat. One chamber was 43.2 cm (17.0 in.) long with a distance of 35.6 cm (14.0 in.) from the injector flange plane to the throat. The other chamber was 33.0 cm (13.0 in.) long with a distance of 25.4 cm (10.0 in.) from the injector flange plane to the throat. The resonator increased the length of the combustion area by an additional 2 cm (0.787 in.). Except for the length of the cylindrical section, all chamber dimensions were the same for both chambers, including the 6.59-cm (2.595-in.) throat diameter.

Figure 3 shows the two calorimeters. The shorter calorimeter contained 26 measuring stations, with the throat location at the 20th station. The longer calorimeter contained 34 stations, with the throat location at the 28th station. The throat station consisted of two circumferential coolant passages, whereas the remaining stations consisted of three circumferential coolant passages. Each station was manifolded with separate inlet and outlet tubes. High-pressure, flexible, water coolant lines connected the vertical pipe manifolds to the axial station connectors which were welded onto the calorimeter chambers. A venturi flowmeter was installed in each inlet tube,

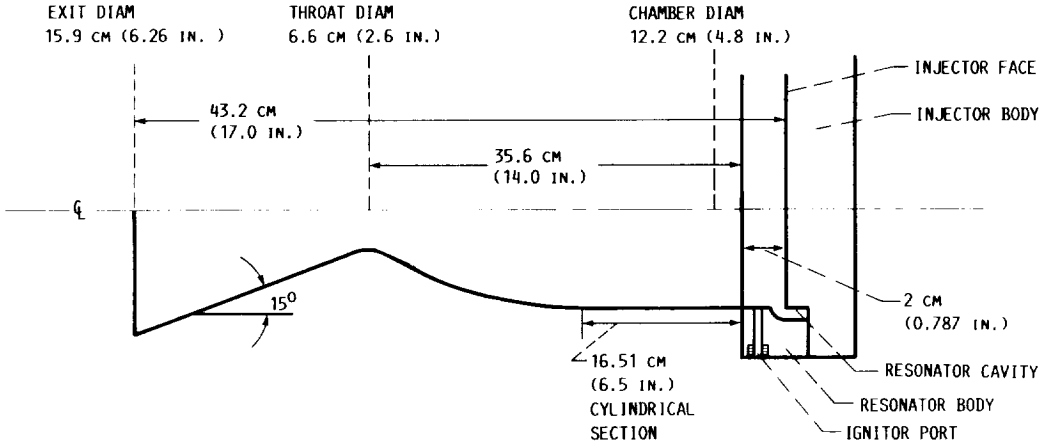

Figure 2.—Long calorimeter chamber dimensions.

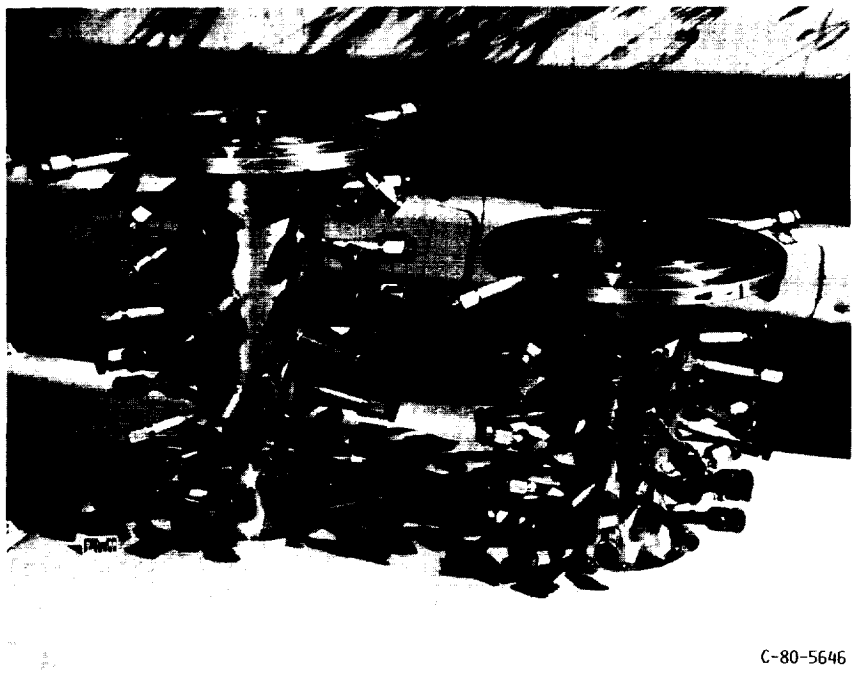

C-80-5646

Figure 3.—Calorimeter chambers.

and a thermocouple was installed in each outlet tube. The circumferential coolant passages allowed individual cooling circuit flow control, which resulted in accurate measurement of heat flux for each station based on the coolant water temperature rise and mass flow rate.

Injector and Resonator

A good injector design provides good propellant mixing, fuel vaporization, and mass flux distribution. To satisfy these requirements, the triplet impinging element injector, which is arranged in an oxidizer-fuel-oxidizer (O–F–O) sequence, was selected. This injector was selected because previous hydrocarbon test work determined that its configuration gave the highest characteristic exhaust velocity efficiency C^*_{eff} of those studied (ref. 5) and because the injector elements were easy to modify. Figure 4(a) shows a triplet impinging element injector that has 37 elements located on a square grid with the elements oriented mutually perpendicular to enhance inter-element mixing. The oxidizer holes are 1.173 cm (0.462 in.) apart (with the fuel hole centered between them) and have an impinging angle of 60° as shown in figure 4(b). Figure 5(a) shows a 61-element triplet injector with 4 radial rings of elements and a central quad element that provides 3 oxidizer streams impinging on a straight fuel stream. Figure 5(b) shows a modification of this injector; the oxidizer elements in the outer triplet ring were closed by electron beam welding, and the fuel holes and inner oxidizer holes were redrilled as showerheads. This pattern provided more fuel in the outer zone, which resulted in film cooling of the chamber wall. More details of the injectors are given in tables I and II.

Figure 6 shows the copper resonator used with the 37-element triplet injector. The resonator contained 16 acoustic cavities evenly arranged around the inside surface of the resonator. The resonator configuration was used during all tests to dampen the chamber acoustic response at potentially unstable modes of combustion.

Test Facility

This program was conducted at the NASA Lewis Research Center Rocket Engine Test Facility. This facility is a 222 400-N (50 000-lbf) sea-level rocket test stand equipped with an exhaust-gas muffler and scrubber. The facility uses pressurized storage tanks to supply the cooling water and propellants to the calorimeter chambers. The propellants were liquid oxygen and ambient temperature RP-1 (kerosene). Details of the facility are shown in figure 7. Figure 7(a) shows the thrust stand above the exhaust-gas scrubber with a typical calorimeter chamber mounted in place. A photograph of the calorimeter chamber (on the test stand) being fired vertically downward is shown in figure 7(b). Figure 7(c) is a schematic of the test facility showing the instrumentation locations and propellant supply lines. Control room operations during testing include monitoring the test hardware by means of three closed-circuit television cameras and one test-cell microphone. The output

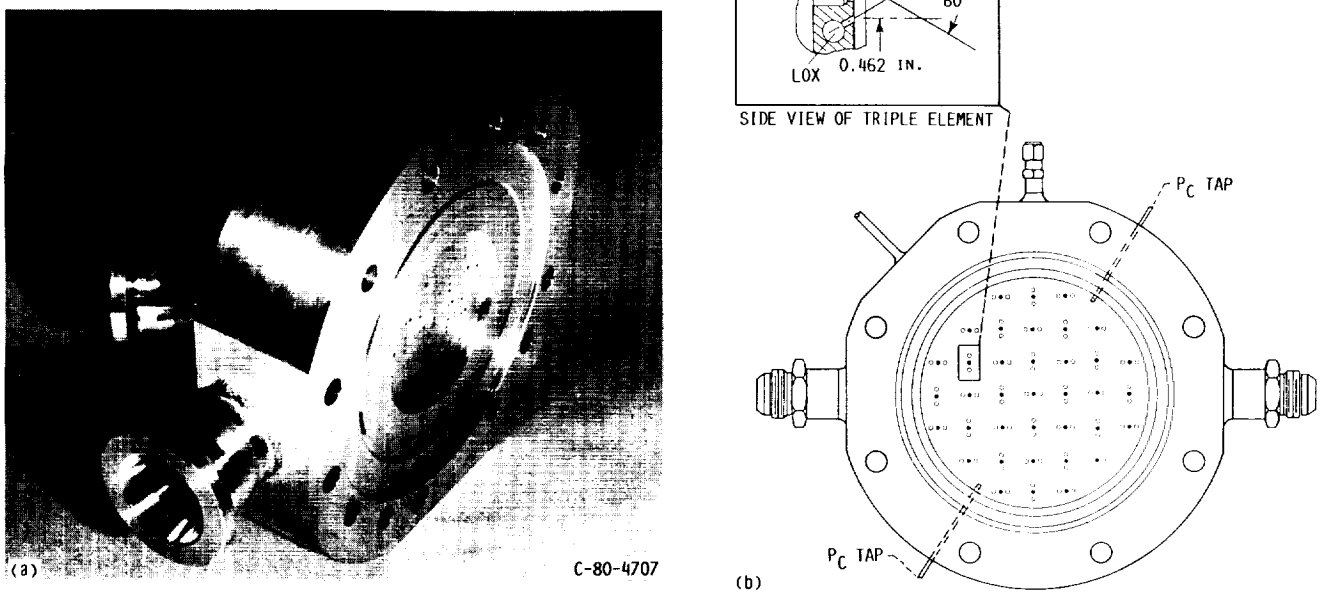

(a) Photograph of 37-element triplet injector.
(b) Sketch of 37-element triplet injector.

Figure 4.—Liquid oxygen/hydrocarbon 37-element triplet injector.

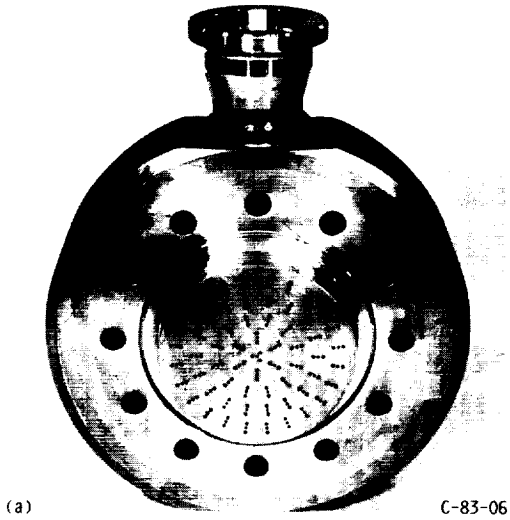

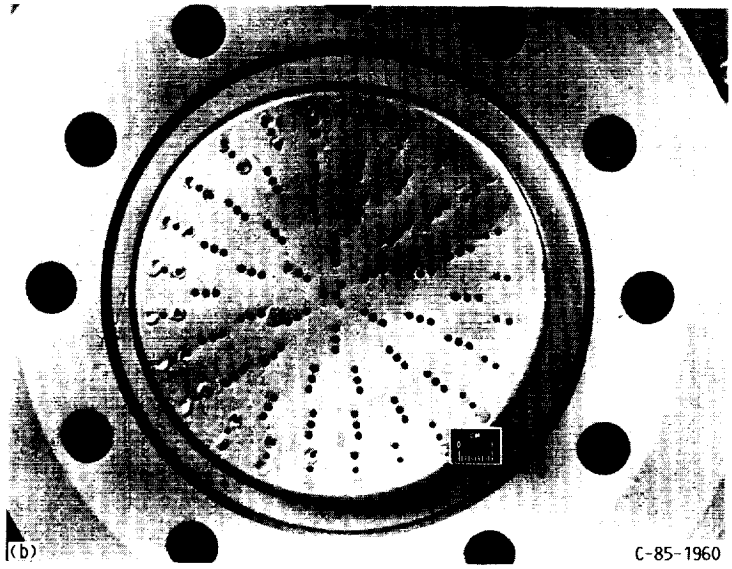

(a) Unmodified injector.
(b) Closeup of modified injector.

Figure 5.—61-Element triplet injector.

TABLE I.—INJECTOR GEOMETRY OF 37-ELEMENT INJECTOR WITH TRIPLET OXYGEN-FUEL-OXYGEN HOLES IN MUTUALLY PERPENDICULAR PATTERN

Injector number	Fuel element		Oxidizer element		Nominal chamber pressure, P_C, MPa abs (psia)
	Hole diameter, mm (in.)	Total flow area, mm^2 ($in.^2$)	Hole diameter, mm (in.)	Total flow area, mm^2 ($in.^2$)	
1	1.702 (0.067)	84.13 (0.1304)	1.489 (0.059)	130.52 (0.2033)	4.1 (600)
2	2.00 (0.078)	114.06 (0.1768)	2.18 (0.086)	277.35 (0.4299)	8.3 (1200)

TABLE II.—INJECTOR GEOMETRY OF 61-ELEMENT INJECTOR WITH TRIPLET OXYGEN-FUEL-OXYGEN TANGENTIAL LIQUID OXYGEN FANS (MODIFIED)

Injector number	Hole diameter, mm (in.)			Flow area, mm^2 ($in.^2$)			Total flow area, mm^2 ($in.^2$)	Portion of total flow in outer zone, percent	Nominal chamber pressure, P_C, MPa abs (psia)
	Outer zone	Core zone	Center zone	Outer zone, 24 holes	Core zone, 36 holes	Center zone, 1 hole			
Fuel element									
3	1.168 (0.046)	1.600 (0.063)	1.600 (0.063)	25.715 (0.040)	72.382 (0.112)	2.011 (0.0031)	100.11 (0.1551)	25.7	8.3 (1200)
4	1.778 (0.070)	2.1844 (0.086)	2.1844 (0.086)	59.587 (0.092)	134.84 (0.209)	3.742 (0.0058)	198.17 (0.3068)	30.0	13.8 (2000)
Oxidizer element									
3	1.168 (0.046)	1.702 (0.067)	1.397 (0.055)	25.735 (0.040)	163.74 (0.254)	4.581 (0.0071)	194.05 (0.3011)	13.2	8.3 (1200)
4	1.575 (0.062)	1.956 (0.077)	1.702 (0.067)	46.75 (0.0725)	216.35 (0.335)	6.825 (0.011)	269.93 (0.4185)	17.3	13.8 (2000)

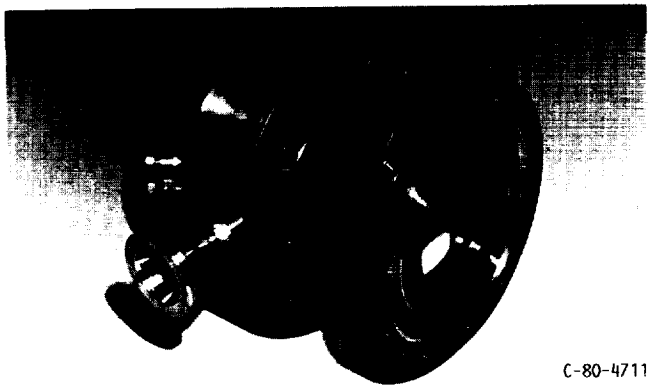

Figure 6.—37-Element triplet injector with resonator ring.

of one television camera and the microphone is recorded on magnetic tape for later playback. A high-speed photographic camera also records each test at a rate of 400 frames/sec.

During each test data are input to an analog-to-digital converter with access to a centrally located IBM 370 computer. Test data are recorded every 0.02 sec and averaged over five recordings, with the average reported every 0.1 sec.

Test Procedure

The experimental calorimeter program consisted of two series of tests. The first series used the short calorimeter, associated water-cooled copper resonator, and the 37-element triplet injectors. The second series used the long calorimeter, associated water-cooled copper resonator, and the 61-element modified triplet injectors.

With the short calorimeter and the low-pressure 37-element injector (injector 1, table I), 7 tests were conducted at an average chamber pressure of 4.32 MPa abs (627 psia) for mixture ratios of 2.4 to 3.0. A single test was then conducted with the high-pressure 37-element injector (injector 2) at a chamber pressure of 8.87 MPa abs (1287 psia) and a mixture ratio of 3.32. A torch igniter, inserted into the combustion area through a port in the resonator, ignited the combustion gases. For all tests the chamber pressure was initially ramped to 1.72 MPa abs (250 psia). After satisfying the safety tolerances, the chamber pressure was ramped to 4.32 MPa abs for the first tests and 8.87 MPa abs for the final test. Between tests processed data were available in the control room by means of a remote terminal with interactive mainframe access. This access allowed review of the processed data prior to the next test.

After review of the short calorimeter data, the long calorimeter was tested with the associated resonator and the original 61-element injector. A very short test was conducted at a mixture ratio of 1.9 and a chamber pressure of 13.5 MPa abs (1962 psia). All further testing was conducted with the modified 61-element injectors (injectors 3 and 4, table II) at three nominal chamber pressures, 4.14, 8.3, and 13.8 MPa abs (600, 1200, and 2000 psia), for mixture ratios of 1.77 to 3.25. The conditions for the test series are given in table III.

Results and Discussion

Tests were conducted to investigate the rocket combustion and heat transfer characteristics of LOX/RP-1 mixtures at high chamber pressures. Two water-cooled calorimeter chambers were tested. The short chamber length was 33.0 cm (13.0 in.),

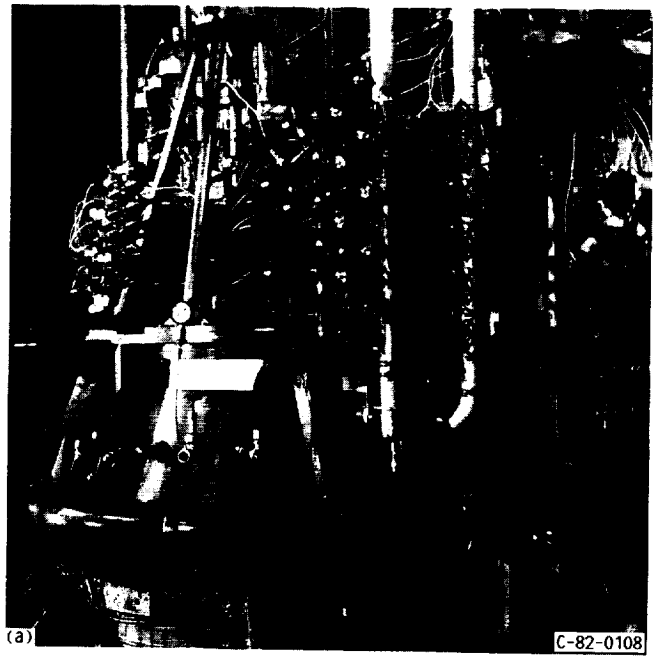

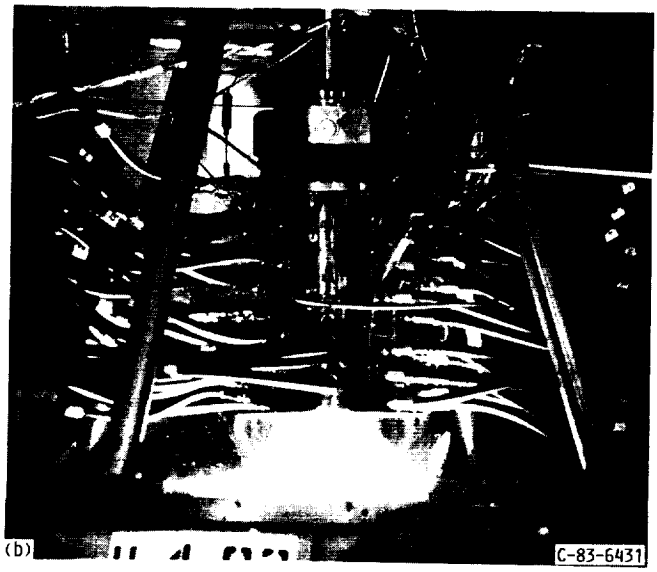

(a) RETF thrust stand with calorimeter in place.
(b) Calorimeter chamber during test firing.

Figure 7.—Rocket Engine Test Facility (RETF) and instrumentation.

INJECTOR PERFORMANCE MEASUREMENT INSTRUMENTATION

Instrument	Location	Measurement
Strain gage bridge load cell	L1	Thrust
Turbine type flow meter	F1	Oxidizer flow
	F2	Oxidizer flow
	F3	Fuel flow
Strain gage bridge pressure transducer	P1	Combustion chamber pressure
	P2	Combustion chamber pressure
	P3	Oxidizer injection pressure
	P4	Fuel injection pressure
	P6	Fuel venturi static pressure
	D1	Oxidizer injection delta pressure
	D2	Fuel injection delta pressure
	D4	Fuel venturi delta pressure
Platinum resistive thermometer	T1	Oxidizer flow meter temperature
	T2	Oxidizer flow meter temperature
	T3	Oxidizer injection temperature
	T4	Fuel injection temperature
Chromel/Constantan thermocouple	T5	Fuel venturi temperature
Flush mounted high frequency piezo-electric pressure transducers	K1	Chamber pressure oscillation
	K2	Chamber pressure oscillation
	K3	Chamber pressure oscillation

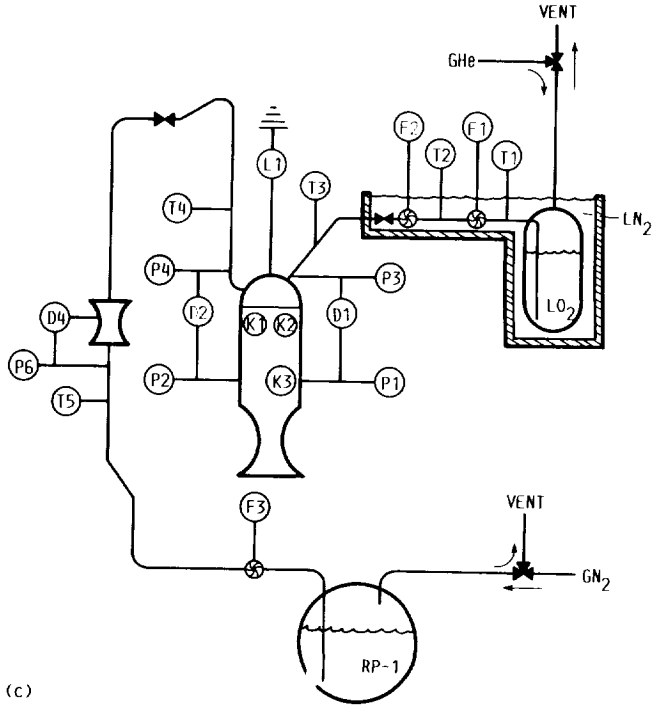

(c) Test facility and instrumentation schematic.

Figure 7.—Concluded.

and the long chamber length was 43.2 cm (17.0 in.). The throat diameter was 6.59 cm (2.595 in.). Heat transfer data were calculated for the various thrust chamber assemblies for comparison with each other and with the data reported in reference 9.

Short Calorimeter with Uniform Mixture Ratio

The short calorimeter was tested with a 37-element O–F–O triplet injector at 2 nominal chamber pressures, 4.32 and

TABLE III.—CALORIMETER TEST CONDITIONS

Run number	Injector number	Nominal chamber pressure, P_C		Run time, sec	Mixture ratio, O/F
		MPa	psia		
Short chamber					
28	1	4.29	622	6.0	2.626
[a]29		4.34	630	6.0	2.795
[a]29		4.33	628	---	3.006
[a]31		4.34	629	6.0	2.860
[a]31		4.31	625	---	2.990
[a]32		4.35	631	6.0	2.386
[a]32		4.32	627	---	2.664
[b]33	2	8.87	1287	1.0	3.324
Long chamber					
[c]43	3	8.16	1184	.3	1.819
44		8.34	1210	1.0	1.916
[c]45		----	----	---	-----
46		8.29	1203	1.0	2.038
47		8.20	1189		2.363
48		7.96	1155		2.708
49		7.90	1146		2.479
[c]50		----	----	---	-----
51		8.29	1202	1.0	2.156
52		7.95	1152	1.0	2.741
[c]53		----	----	---	-----
54		8.03	1165	1.0	2.888
55		8.11	1177	1.0	2.922
[d]56	4	13.53	1962	.3	1.921
57		13.89	2015	.3	1.769
58		13.90	2016	1.0	2.003
59		14.14	2051		2.088
60		13.34	1935		2.529
61		14.04	2036		2.364
62		13.42	1947		2.786
63		13.53	1962		1.885
64		13.50	1958		2.743
[c]65	3	----	----	.2	-----
66		3.36	488	.2	2.098
67		4.29	622	1.3	1.996
68		4.11	597		2.428
69		4.15	603		2.693
70		4.18	607		2.233
71		3.41	495		3.073
72		4.12	598		2.977
73		3.96	574		3.249
74		4.14	600		2.609

[a]Two data points were taken from the run.
[b]Thrust chamber, resonator, and injector destroyed.
[c]Test aborted.
[d]Unmodified version of injector 4 was used. The injector was destroyed.

8.87 MPa abs (627 and 1287 psia). All testing was done for steady-state conditions and with a uniform mixture ratio. Seven data points were acquired at a nominal chamber pressure of 4.32 MPa abs for mixture ratios ranging from 2.39 to 3.01. A single data point was acquired at a nominal chamber pressure of 8.87 MPa abs and a mixture ratio of 3.32. The heat transfer per unit area Q/A at the chamber throat for these data points is shown as a function of mixture ratio in figure 8. The heat transfer rate Q is calculated from the cooling water temperature rise and the mass flow rate

$$Q = \dot{m}C_p(T_{ce} - T_{ci}) \tag{1}$$

For comparison purposes a second point, for a nominal chamber pressure of 8.87 MPa abs at a mixture ratio of 2.55, was projected from the 4.32 MPa abs data. The heat flux at 4.32 MPa abs was scaled up to 8.87 MPa abs by using the relationship (ref. 7)

$$\frac{Q}{A} \propto (P_C)^{0.8}$$

or

$$\frac{\left(\frac{Q}{A}\right)_1}{\left(\frac{Q}{A}\right)_2} = \left(\frac{P_{C1}}{P_{C2}}\right)^{0.8} \tag{2}$$

This relationship gave a projected heat flux of 6.4 kW/cm^2 (39.6 Btu/in.^{2} sec).

The experimental data from this test series was scaled up (by using eq. (2)) from a nominal chamber pressure of 4.32 MPa abs to a nominal chamber pressure of 13.65 MPa abs (1980 psia) over a range of mixture ratios from 1.9 to 2.8. Comparison with the experimental data reported in reference 9 showed that the scaled-up data fell 11.5 percent below the reference 9 data at a mixture ratio of 2.8 and that at a mixture ratio of 2.4 the difference was 12.9 percent. A change in the heat flux of this magnitude could be a result of the type of injector. An O–F–O impinging 37-element injector (fig. 4(a)) was used to obtain the NASA data. A preatomized triplet injector that had fuel-oxidizer-fuel (F–O–F) elements was used to obtain the reference 9 data. Since similar chamber contours were used upstream of the throat, the difference between the two injectors could explain the 11.5 percent to 12.9 percent variations in heat flux data. There was a good correlation between the 4.32 MPa abs data and the 8.87 MPa abs data because the same type of injector was used (injectors 1 and 2 in table I).

Heat flux profiles for several mixture ratios are shown in figure 9. Figure 9(a) presents the NASA data, and figure 9(b)

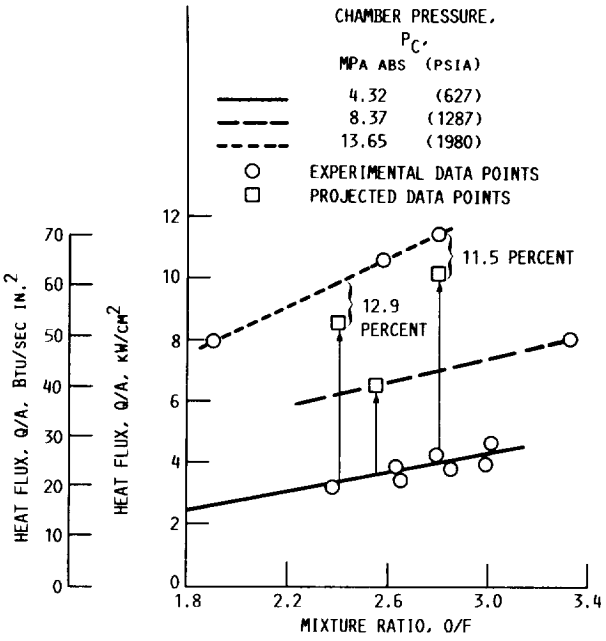

Figure 8.—Throat section heat flux data for uniform mixture ratio combustion.

presents data from reference 9. Curves I and II in figure 9(a) represent experimental data at a nominal chamber pressure of 4.32 MPa abs. Curve III is a projection of the data of curve II at a mixture ratio of 3.32. Curve IV is the experimental data at a nominal chamber pressure of 8.87 MPa abs and a mixture ratio of 3.32. Comparison of curves III and IV shows that the data follow the relationship $Q/A \propto (P_C)^{0.8 \text{ to } 1.0}$ in the combustion section of the chamber, and the relationship $Q/A \propto (P_C)^{0.7 \text{ to } 0.8}$ in the divergent and throat sections of the chamber.

The plots in figure 9(b) are at a nominal chamber pressure of 13.65 MPa abs for several other mixture ratios. The experimental heat flux is approximately 60 percent higher at the throat than the design prediction. By using equation (2), curve I of figure 9(a) was scaled up to 13.65 MPa abs and a mixture ratio of 2.80 for comparison with the reference 9 data at the same pressure and mixture ratio (see fig. 9(c)). The NASA data agree with the reference 9 data (fig. 9(c)) in that the experimental heat flux is approximately 60 percent higher than the design prediction of reference 9. The variations upstream of the throat indicate that the injector characteristics affect the heat flux until combustion is complete. Because the two chambers have different geometries in the divergent section, the heat flux profiles decline at different rates.

Carbon Deposits with Uniform Mixture Ratio

One interesting characteristic that extends over the mixture ratio range tested is the development of carbon deposits (soot) along the calorimeter wall. The carbon layer thickness appears to vary with axial location at a chamber pressure of 4.14 MPa abs (600 psia). The heat transfer coefficient for a soot-coated chamber was calculated by using the following equations:

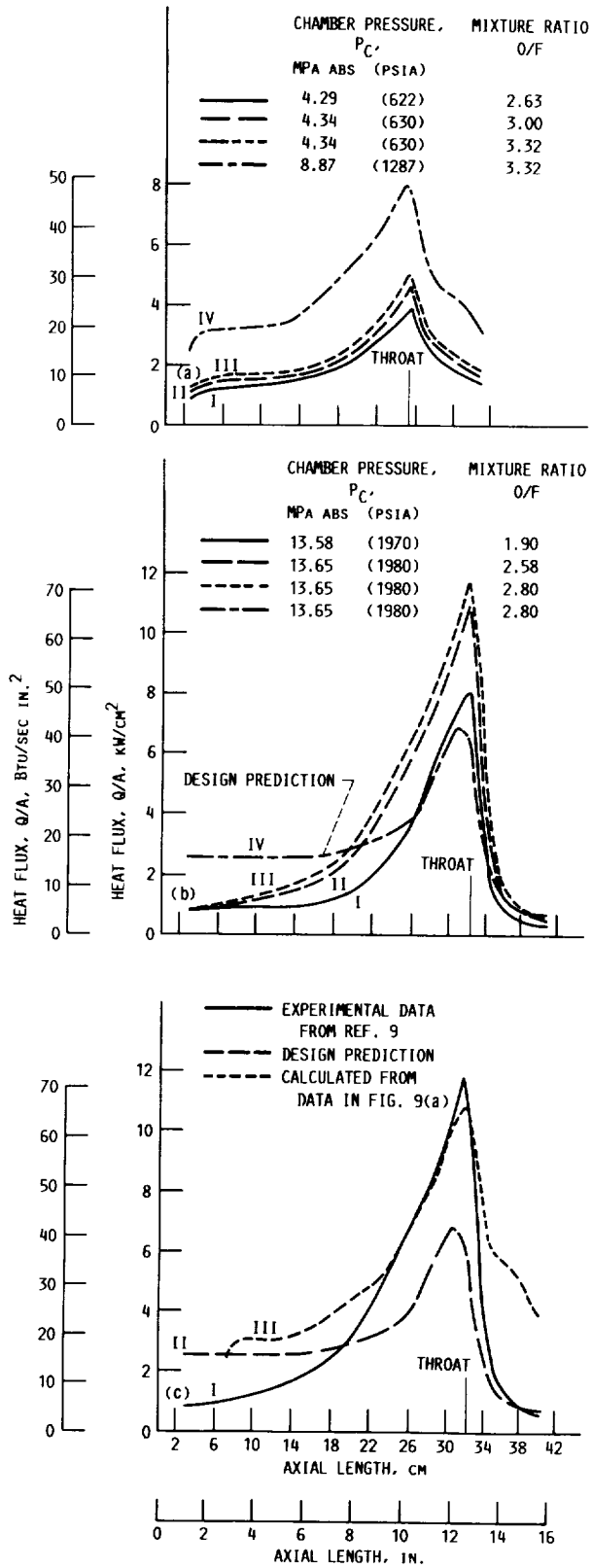

(a) Data from short calorimeter with uniform mixture ratio.
(b) Data from reference 9 calorimeter.
(c) Comparison of data at 2.8 mixture ratio and 13.65-MPa abs (1980-psia) chamber pressure.

Figure 9.—Heat flux along calorimeter axial length.

$$h_g = \frac{1}{R_g + R_d} \tag{3}$$

and

$$\frac{Q}{A} = h_g(T_{aw} - T_{gw}) \tag{4}$$

or

$$(h_g)_{\text{UMR}} = \frac{\left(\frac{Q}{A}\right)_{\text{UMR}}}{(T_{aw} - T_{gw})_{\text{UMR}}} \tag{4a}$$

where R_g is the combustion gas resistance, R_d is the carbon deposit resistance, T_{aw} is the adiabatic wall temperature, and T_{gw} is the combustion-gas-side wall temperature. The heat flux Q/A was obtained from the experimental data of the lower line in figure 8 and T_{gw} is calculated from the heat transfer through the metal wall of thickness X by assuming no axial conduction (one-dimensional heat transfer)

$$\frac{Q}{A} = \frac{k_m}{X}(T_{gw} - T_{cw}) \tag{5}$$

or

$$T_{gw} = \frac{QX}{Ak_m} + T_{cw} \tag{5a}$$

where k_m is the metal wall conductivity and T_{cw} is the coolant-side wall temperature. To determine T_{cw}, an initial value for the coolant-side wall temperature T_{wc} is assumed, and a coolant heat transfer coefficient h_c is calculated from the equation

$$h_c = \frac{0.019}{d} k_f (\text{Re})_f^{0.8} (\text{Pr})_f^{0.4} \tag{6}$$

where the film conductivity k_f, film Reynolds number $(\text{Re})_f$, and the film Prandtl number $(\text{Pr})_f$ are evaluated for a film temperature T_{cf} equal to $(T_c + T_{wc})/2$ (ref. 10). Then the coolant-side wall temperature T_{cw} is evaluated from the heat transfer equation,

$$\frac{Q}{A} = h_c(T_{cw} - T_c) \tag{7}$$

which can be restated as

$$T_{cw} = \frac{Q}{Ah_c} + T_c \tag{7a}$$

T_{cw} and h_c are iterated in equations (6) and (7a) until $T_{cw} = T_{wc}$. To solve equation (4) for h_g, T_{aw} is calculated by using the following equation (ref. 11):

$$T_{aw} = T_s + \delta_a(T_o - T_s) \tag{8}$$

The adiabatic recovery factor δ_a is taken as 0.88, and the static temperature T_s is calculated from one-dimensional equilibrium theory. The total temperature T_o was calculated as follows:

$$T_o = (C^*_{\text{eff}})^2 (T_o)_{\text{ODE}} \tag{9}$$

where $(T_o)_{\text{ODE}}$ is the one-dimensional total temperature. With injectors 1 and 2, however, the C^*_{eff} is experimentally found to be 99.5 percent. Therefore, the effect on h_g is negligible when $(T_o)_{\text{ODE}}$ replaces T_o.

An empirical expression (ref. 7) for R_d based on the mass velocity of the propellant flow G is

$$R_d = e^{(11.7-7.26G)} (\text{cm}^2 \text{ sec K/kcal})$$

or

$$R_d = e^{(9.0-0.51G)} (\text{in.}^2 \text{ sec } ^\circ\text{R/Btu}) \tag{10}$$

From these equations the combustion gas resistance R_g can be calculated. A comparison can then be made between a soot-coated chamber and a soot-free chamber. The lower line in figure 10 shows the soot-coated throat heat transfer coefficient as a function of mixture ratio at a nominal chamber pressure of 4.32 MPa abs (627 psia). The upper line is the estimated heat transfer coefficient for a soot-free chamber under the same conditions. The heat transfer coefficient decreases by approximately 40 percent for the soot-coated chamber compared with a soot-free chamber.

Long Calorimeter with Nonuniform Mixture Ratio

Reduction in heat flux can be achieved by increasing the fuel flow in the outer zone of injector elements. The outer zone can be run at a mixture ratio below the nominal injector mixture ratio while the core elements are run slightly above the nominal injector mixture ratio. In theory, this procedure provides a lower temperature combustion gas along the wall and a higher temperature combustion gas in the core flow (ref. 7).

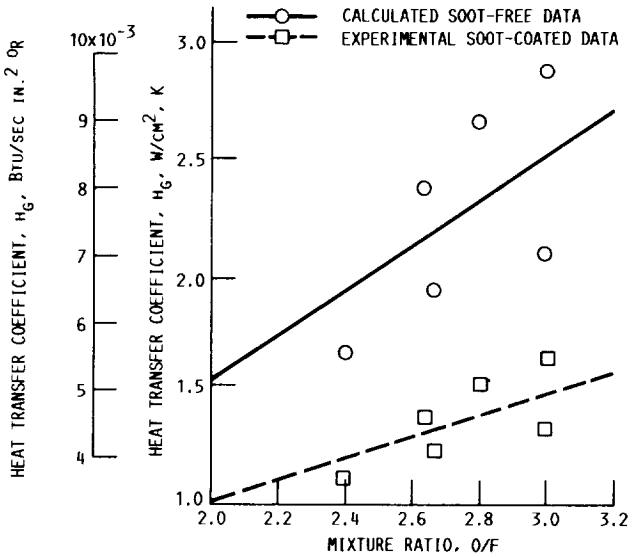

Figure 10.—Throat heat transfer coefficient as a function of mixture ratio for the uniform mixture ratio injector at 4.32-MPa abs (627-psia) chamber pressure.

The 61-element O–F–O triplet injector shown in figure 5(a) was modified (fig. 5(b)) in order to acquire heat flux data for zoned combustion. By sealing the outer oxidizer holes, the combustion gas adjacent to the chamber wall became fuel-rich and functioned as a protective thermal barrier. For large thrust chambers, the propellant mixture ratio of the core flow was not altered significantly when the outer zone flow was fuel-rich (ref. 7). However, with small thrust chambers, such as the ones used in this program, the core mixture ratio had to be significantly increased because the outer zone included a significant amount of the mass flow. The outer zone in these chambers provided 26 to 30 percent of the total fuel mass flow rate and 13 to 17 percent of the total oxidizer mass flow rate.

The heat flux as a function of mixture ratio for zoned combustion is shown in figure 11. Figure 11(a) shows the heat flux in the combustion area near the injector. The bottom curve is a best fit for the experimental data at a nominal chamber pressure of 4.14 MPa abs (600 psia). The middle curve is a best fit for the experimental data at a nominal chamber pressure of 8.3 MPa abs (1200 psia), and similarly the top curve, at 13.8 MPa abs (2000 psia). Figure 11(b) to (d) shows the heat flux in the chamber at the following locations: in the convergent section just before the throat (fig. 11(b)), in the throat section (fig. 11(c)), and in the divergent section downstream of the throat (fig. 11(d)). On all parts of the figure, the slopes of the best fit curves for the heat flux are nearly the same for the 8.3 and 13.8 MPa abs chamber pressures. However, the best fit curve for heat flux is much flatter at 4.14 MPa abs than at the higher chamber pressures. A possible explanation for the different slopes could be that at a chamber pressure of 4.14 MPa abs, injector 3, which was designed for a chamber pressure of 8.3 MPa abs, was used.

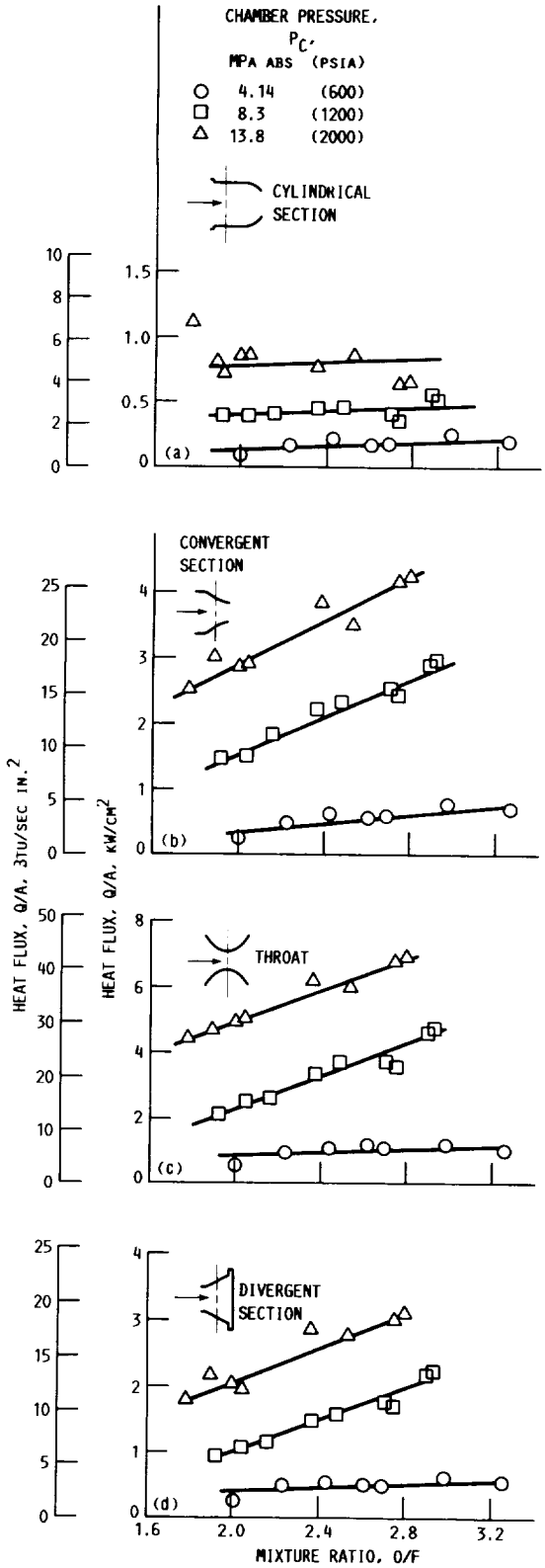

(a) At cylindrical section.
(b) At convergent section.
(c) At throat section.
(d) At divergent section.

Figure 11.—Heat flux data with zoned combustion.

Carbon Deposits with Nonuniform Mixture Ratio

Heat transfer coefficients as a function of the core flow mixture ratio were also derived for the modified injector. The equations used for the heat transfer coefficient were

$$h_g' = \frac{1}{R_k + R_z + R_d} \tag{11}$$

and

$$h_g' = \frac{\left(\frac{Q}{A}\right)'}{(T_{aw} - T_{gw})'} \tag{12}$$

where R_k is the core resistance, R_z is the outer zone resistance, and R_d is the carbon deposit resistance. In equation (12), the heat flux, $(Q/A)'$, is obtained from figure 11(c) for the designated core mixture ratio. The adiabatic wall temperature T_{aw} was calculated from the same equations used for the uniform mixture flow

$$T_{aw} = T_s + \delta_a(T_o - T_s) \tag{8}$$

$$T_o = (C_{\text{eff}}^*)^2 \, (T_o)_{\text{ODE}} \tag{9}$$

The modified injector provided an average C_{eff}^* of 96.3 percent at 13.8 MPa abs (1200 psia), which was used in equation (9). By using the empirical expression (ref. 7) for R_d, equation (10), the combined resistance $(R_k + R_z)$ can be calculated. A comparison can then be made between a soot-coated chamber and a soot-free chamber. The lower line of figure 12 shows the soot-coated throat heat transfer coefficient as a function of mixture ratio at a nominal chamber pressure of 13.8 MPa abs (2000 psia). The upper line is the estimated heat transfer coefficient for a soot-free chamber. The heat transfer coefficient decreases by approximately 60 percent for the soot-coated chamber compared with the soot-free chamber.

Comparison of Zoned and Uniform Mixture Ratio Combustion

A comparison of engine systems with zoned and uniform mixture ratio combustion is shown in figure 13. In figure 13(a), plot I shows the heat flux distribution over the axial length of the short calorimeter for a nominal chamber pressure of 8.87 MPa abs (1287 psia). The 37-element injector that was used with the short calorimeter to obtain these data (injector 2) provided a uniform mixture ratio of 3.32. Plot II shows the heat flux distribution over the axial length of the long calorimeter for a nominal chamber pressure of 8.11 MPa abs (1177 psia) and an overall mixture ratio of 2.93. Plot III shows the heat flux distribution over the axial length of the long calorimeter for a nominal chamber pressure of 8.34 MPa abs (1210 psia) and an overall mixture ratio of 2.03. The data for plots II and III were obtained by using the 61-element injector

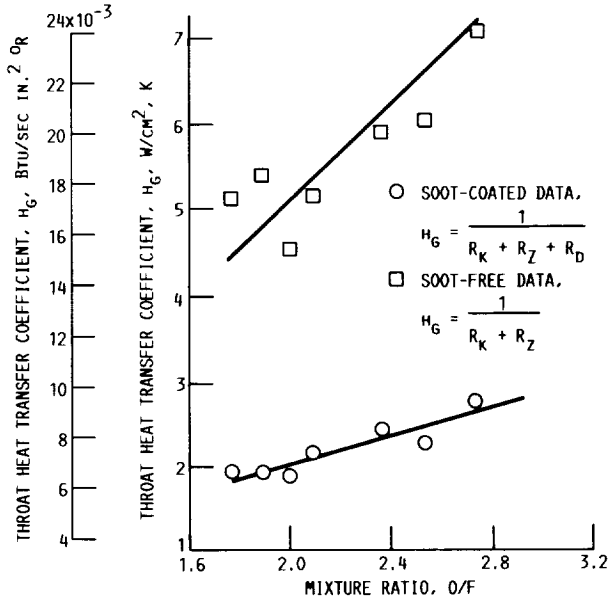

Figure 12.—Throat heat transfer coefficient as a function of mixture ratio for modified injector at 13.8-MPa abs (2000-psia) chamber pressure.

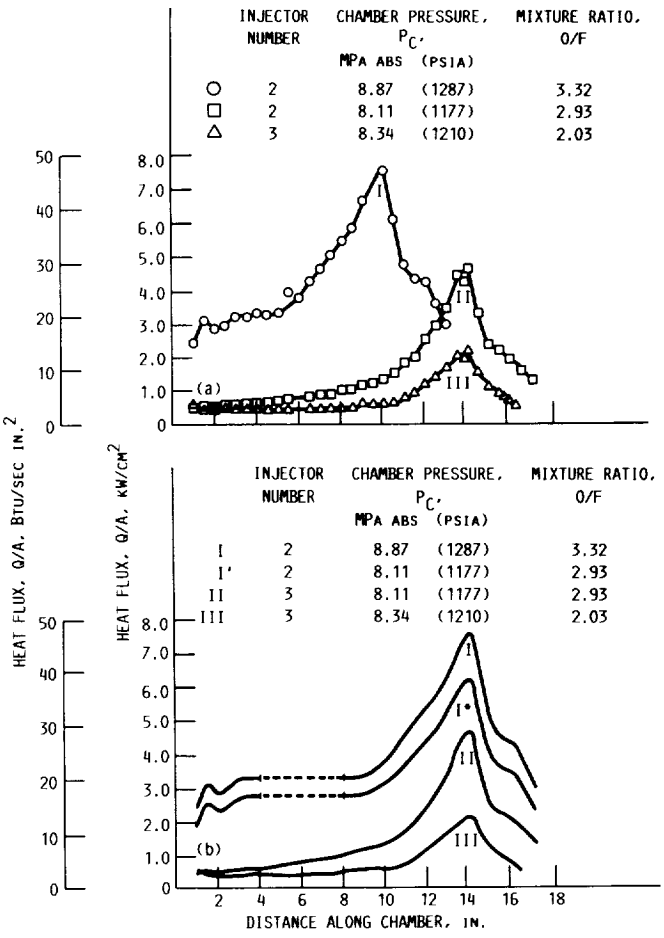

(a) Heat flux distribution for unmodified and modified injectors.
(b) Total heat flux comparison for equivalent length.

Figure 13.—Comparison of heat flux for 61-element zoned combustion (injector 3) and 37-element uniform mixture ratio combustion (injector 2).

with zoned combustion (injector 3). The heat flux over the entire calorimeter surface area was 4262 kW (4040 Btu/sec) for plot I, 1860 kW (1760 Btu/sec) for plot II, and 950 kW (900 Btu/sec) for plot III. With the addition of 10.2 cm (4.0 in.) to the cylindrical section for an equivalent length comparison, the total heat flux for plot I in figure 13(a) became 4830 kW (4575 Btu/sec), which is shown in figure 13(b) as plot I. When projected to match the chamber pressure P_C and mixture ratio O/F for the test represented by plot II, the total heat flux for plot I became 3491 kW (3309 Btu/sec) as shown in plot I*. The formula $(P_C)^{0.8}(O/F)_{II}/(O/F)_I$, where O/F_{II} is the mixture ratio of plot II and $(O/F)_I$ is the mixture ratio of plot I, was used for the evaluation of heat flux at the throat and downstream of the throat. The formula $(P_C)(O/F)_{II}/(O/F)_I$ was used upstream of the throat. The total heat flux for plot II for zoned combustion over the entire calorimeter area is 53 percent of the total heat flux for uniform mixing.

A comparison of C^*_{eff} for the unmodified and modified injectors is shown in figure 14. Horizontal lines are plotted for each test series as a best fit of the experimental data. The top line shows the results for the 4.14 MPa abs (600 psia) tests with injector 1. The projected best fit line gives a C^*_{eff} of approximately 99.5 percent. The lower lines show the results with injectors 3 and 4. The best fit lines indicate C^*_{eff} of 95 to 96.2 percent over the mixture ratio range. When comparing the injector modified for zoned flow with the injector designed for uniform flow, a reduction in heat flux of 47 percent was achieved in the throat region with only a 4.5 percent reduction in C^*_{eff}.

Heat Flux Ratio of Zoned Combustion to Uniform Mixing Combustion

For a given chamber contour, a relationship can be established between the heat flux for a nonuniform mixture ratio (zoned) and a uniform mixture ratio (UMR) combustion. The following procedure was used to determine the ratio of the heat flux for nonuniform mixing to uniform mixing combustion. The rate of heat transfer Q to the wall is a function of the combustion gas heat transfer coefficient h_g, the area over which heat is being transferred A, and the difference between the adiabatic wall temperature T_{aw} and the combustion-gas-side wall temperature T_{gw}

$$\frac{Q}{A} = h_g(T_{aw} - T_{gw}) \tag{4}$$

Equation (4) can be solved for the uniform mixture ratio combustion gas heat transfer coefficient,

$$(h_g)_{UMR} = \frac{\left(\frac{Q}{A}\right)_{UMR}}{(T_{aw} - T_{gw})_{UMR}} \tag{4a}$$

Similarly, the zoned combustion gas heat transfer coefficient, h_g', can be written as

$$h_g' = \frac{\left(\frac{Q}{A}\right)'}{(T_{aw} - T_{gw})'} \tag{12}$$

The ratio $(Q/A)'/(Q/A)$, which represents the reduction in heat transfer to the wall because of fuel-rich zoned combustion, can be determined by rearranging equations (4a) and (12):

$$\frac{\left(\frac{Q}{A}\right)'}{\left(\frac{Q}{A}\right)_{UMR}} = \frac{h_g'(T_{aw} - T_{gw})'}{(h_g)_{UMR}(T_{aw} - T_{gw})_{UMR}} \tag{13}$$

or

$$\frac{\left(\frac{Q}{A}\right)'}{\left(\frac{Q}{A}\right)_{UMR}} = \frac{\left(\frac{Q}{A}\right)'}{(h_g)_{UMR}(T_{aw} - T_{gw})_{UMR}} \tag{13a}$$

The heat flux ratio for the geometric configuration in figure 2 can be determined by comparing figure 11(c) data with figure 8 data, as shown in figure 15. For a chamber pressure of 8.3 MPa abs (1200 psia), the heat flux ratio increases over the entire mixture ratio range. However, at 4.14 MPa abs (600

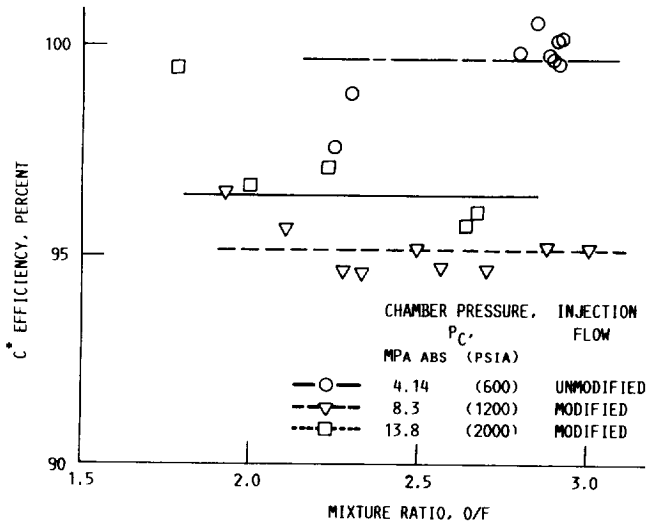

Figure 14.—Injector performance determined by characteristic exhaust velocity efficiency.

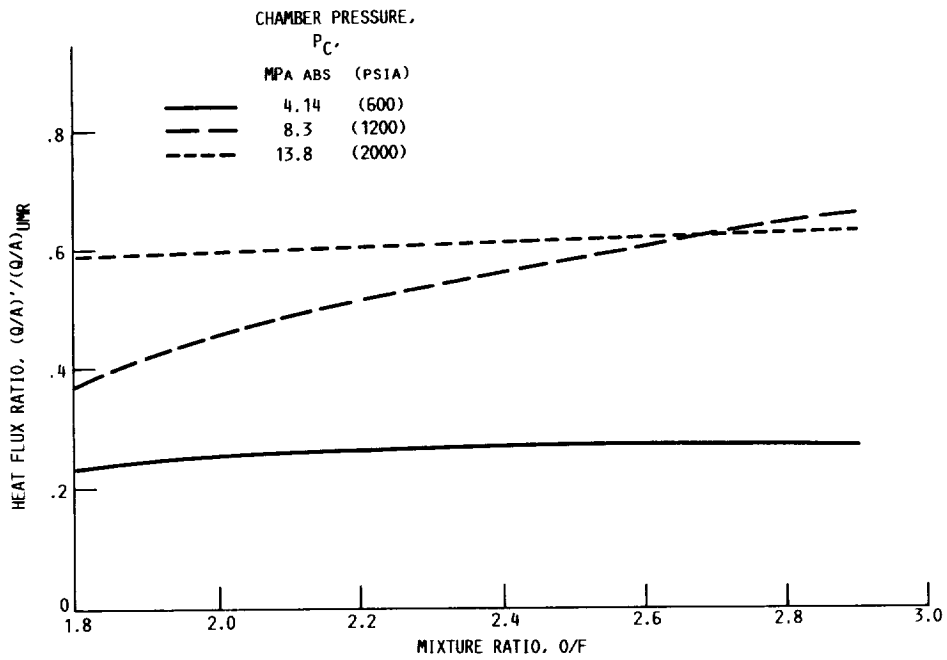

Figure 15.—Ratio of heat flux of zoned mixing combustion to that of uniform mixing combustion at throat.

psia) and 13.8 MPa abs (2000 psia) chamber pressure, a change in mixture ratio has no noticeable effect on the heat flux ratio.

Concluding Remarks

This program has shown that heat transfer from the combustion gases to the chamber wall can be dramatically reduced through zoned combustion. Zoned combustion provides a lower temperature combustion gas along the wall, which reduces the wall temperature. Consequently, the life of the chamber will be increased because of the reduction in thermal strain in the wall. The wall temperature is also reduced through the formation of carbon deposits on the wall which act like a thermal barrier coating. Therefore, zoned combustion and the formation of carbon deposits on the wall should be considered beneficial, from a heat transfer perspective, to long-term operation of a hydrocarbon-fueled rocket engine.

Summary of Results

This test program investigated the rocket combustion and heat transfer characteristics of LOX/RP-1 mixtures at high chamber pressures by using two water-cooled calorimeters. The short, water-cooled calorimeter chamber (33.0 cm) was tested with 37-element O-F-O triplet injectors, and the long, water-cooled calorimeter chamber (43.2 cm) was tested with 61-element O-F-O triplet injectors. The short chamber was tested at 4.14- and 8.3-MPa abs (600- and 1200-psia) nominal chamber pressures. The long chamber was tested at 4.14-, 8.3-, and 13.8-MPa abs (600-, 1200-, and 2000-psia) nominal chamber pressures. Heat flux Q/A data were obtained over the entire calorimeter length for mixture ratios ranging from 1.77 to 3.32. Test data at 4.14 MPa abs were compared with data from another source. Injector modifications were made to evaluate the effect of a fuel-rich outer zone on the heat transfer rate and the characteristic exhaust velocity efficiency C^*_{eff}.

A summary of the test program results are as follows:

1. The 37- and 61-element O-F-O injectors with associated resonators provided stable combustion for the water-cooled calorimeter chambers tested with LOX/RP-1 mixture ratios ranging from 1.77 to 3.32.

2. The uniform mixture ratio data from this test program agree with cited data in that the experimental heat flux at the throat was approximately 60 percent higher than the design prediction.

3. With uniform propellant mixing at a nominal chamber pressure of 4.14 MPa abs, the hot-gas-side heat transfer coefficient decreased by approximately 40 percent for a soot-coated chamber when compared with a soot-free chamber.

4. With fuel-rich zoned combustion, the hot-gas-side, soot-coated, throat heat transfer coefficient at 13.8 MPa abs was approximately 60 percent less than the soot-free throat heat transfer coefficient.

5. When comparing the fuel-rich zoned combustion to uniform combustion at a nominal chamber pressure of 8.3 MPa abs, a reduction in heat flux of 47 percent was achieved in the throat region with only a 4.5-percent reduction in C^*_{eff}.

Lewis Research Center
National Aeronautics and Space Administration
Cleveland, Ohio, August 15, 1988

References

1. Luscher, W.P.; and Mellish, J.A.: Advanced High Pressure Engine Study for Mixed-Mode Vehicle Applications. NASA CR-135141, 1977.
2. Haefeli, R.C.; et al: Technology Requirement for Advanced Earth-Orbital Transportation Systems. NASA CR-2866, 1977.
3. Hepler, A.K.; and Bangsund, E.L.: Technology Requirements for Advanced Earth Orbital Transportation System. NASA CR-2878, 1978.
4. Calouri, V.A.; Conrad, R.T.; and Jenkins, J.C.: Technology Requirements for Future Earth-to-Geosynchronous Orbit Transportation Systems. NASA CR-3265, 1980.
5. Pavli, A.J.: Design and Evaluation of High Performance Rocket Engine Injectors for Use with Hydrocarbon Fuels. NASA TM-79319, 1979.
6. Price, H.G.; and Masters, P.A.: Liquid Oxygen Cooling of High Pressure LOX/Hydrocarbon Rocket Thrust Chambers. NASA TM-88805, 1986.
7. Cook, R.T.: Advanced Cooling Techniques for High Pressure Hydrocarbon-Fueled Engines. (RI/RD79-310, Rockwell International Corp.; NASA Contract NAS3-21381) NASA CR-159790, 1979.
8. Frankenfeld, J.W.; et al: High Performance, High Density Hydrocarbon Fuels. (Exxon/GRUS.1KWD.78, Exxon Research and Engineering Co.; NASA Contract NAS3-20394) NASA CR-159480, 1978.
9. Labotz, R.J.; Rousar, D.C.; and Valler, H.W.: High-Density Fuel Combustion and Cooling Investigation. NASA CR-165177, 1980.
10. Swenson, H.S.; Kakarala, C.R.; and Carver, J.R.: Heat Transfer to Supercritical Water in Smooth-Bore Tubes. J. Heat Trans., vol. 87, no. 4, Nov. 1965, pp. 477-484.
11. Curren, A.N.; Price, H.G. Jr.; and Douglass, H.W.: Analysis of Effects of Rocket-Engine Design Parameters on Regenerative-Cooling Capabilities of Several Propellants. NASA TN D-66, 1959.

NASA
National Aeronautics and Space Administration

Report Documentation Page

1. Report No.	2. Government Accession No.	3. Recipient's Catalog No.
NASA TP-2862		

4. Title and Subtitle
High-Pressure Calorimeter Chamber Tests for Liquid Oxygen/Kerosene (LOX/RP-1) Rocket Combustion

5. Report Date
December 1988

6. Performing Organization Code

7. Author(s)
Philip A. Masters, Elizabeth S. Armstrong, and Harold G. Price

8. Performing Organization Report No.
E-2645

10. Work Unit No.
582-01-11

9. Performing Organization Name and Address
National Aeronautics and Space Administration
Lewis Research Center
Cleveland, Ohio 44135-3191

11. Contract or Grant No.

13. Type of Report and Period Covered
Technical Paper

12. Sponsoring Agency Name and Address
National Aeronautics and Space Administration
Washington, D.C. 20546-0001

14. Sponsoring Agency Code

15. Supplementary Notes

16. Abstract

An experimental program was conducted to investigate the rocket combustion and heat transfer characteristics of liquid oxygen/kerosene (LOX/RP-1) mixtures at high chamber pressures. Two water-cooled calorimeter chambers of different combustion lengths were tested using 37- and 61-element oxidizer-fuel-oxidizer triplet injectors. The tests were conducted at nominal chamber pressures of 4.1, 8.3, and 13.8 MPa abs (600, 1200, and 2000 psia). Heat flux Q/A data were obtained for the entire calorimeter length for oxygen/fuel mixture ratios of 1.8 to 3.3. Test data at 4.1 MPa abs compared favorably with previous test data from another source. Using an injector with a fuel-rich outer zone reduced the throat heat flux by 47 percent with only a 4.5 percent reduction in the characteristic exhaust velocity efficiency C^*_{eff}. The throat heat transfer coefficient was reduced approximately 40 percent because of carbon deposits on the chamber wall.

17. Key Words (Suggested by Author(s))	18. Distribution Statement
Heat transfer LOX/RP-1 rocket combustion Calorimeter chamber tests Rocket injectors	Unclassified – Unlimited Subject Category 20

19. Security Classif. (of this report)	20. Security Classif. (of this page)	21. No of pages	22. Price*
Unclassified	Unclassified	15	A03

NASA FORM 1626 OCT 86

*For sale by the National Technical Information Service, Springfield, Virginia 22161

NASA-Langley, 1988